High-Gain-Observer-Based Integral Sliding Mode Control for Position Tracking of Electrohydraulic Servo Systems

Daehee Won, *Member, IEEE*, Wonhee Kim, *Member, IEEE*, and Masayoshi Tomizuka, *Life Fellow, IEEE*

***Abstract*—Although previous control methods improve control performance in electrohydraulic servo system (EHSS), they require full-state feedback information and/or the derivative of the measured signals so that noise may be amplified. In this paper, we propose a high-gain-observer-based integral sliding mode control to improve the position tracking performance of the EHSSs while solving the previous problems. The proposed method consists of a high-gain observer and an integral sliding mode controller. The high-gain observer is designed to estimate the velocity and load pressure using the position feedback. The stability is proven without the approximation of the model in EHSS. The integral sliding mode controller is proposed to improve the position tracking performance using the flatness property of the system. In the controller, the required derivatives of the state variables are obtained using the flatness property without employing the derivative of the measured signal.**

***Index Terms*—Electrohydraulic servo system (EHSS), flatness, observer, position tracking control.**

NOMENCLATURE

x_p	Piston position [m].
x_v	Spool position of the servo-valve [m].
P_A	Pressure of chamber A [N/m^2].
P_B	Pressure of chamber B [N/m^2].
$P_L = P_A - P_B$.	Differential pressure between chambers A and B [N/m^2].
i_v	Input current of the torque motor [mA].
k_v	Gain between spool position and current of the servo valve [m/mA].
Q_L	Load flow rate of the servo valve [m^3/s].
C_d	Discharge coefficient.
w	Area gradient of the servo-valve spool [m].
P_s	Supply pressure of the servo valve [N/m^2].
ρ	Density of hydraulic oil [kg/m^3].
A_p	Pressure area of the piston [m^2].
C_{il}	Internal leakage coefficient [m^5/Ns].
C_{el}	External leakage coefficient [m^5/Ns].
$C_{tl} = C_{il} + \frac{C_{el}}{2}$	Total leakage coefficient [m^5/Ns].
V_t	Total actuator volume [m^3].
β_e	Effective bulk modulus of the hydraulic fluid [N/m^2].
m	Constant mass of the piston and the load [kg].
k	Load spring constant [N/m].
b	Viscous friction coefficient [N/(m/s)].

Manuscript received December 19, 2016; revised April 7, 2017, June 22, 2017, and August 18, 2017; accepted October 1, 2017. Date of publication October 17, 2017; date of current version December 13, 2017. Recommended by Technical Editor M. Basin. This work was supported in part by the Basic Science Research Program through the National Research Foundation of Korea funded by the Ministry of Education under Grant NRF-2016R1C1B1014831, and in part by the Korea Institute of Industrial Technology as "Development of Soft Robotics Technology for Human-Robot Coexistence Care Robots (KITECH EO170045)." *(Corresponding author: Wonhee Kim.)*

D. Won is with the Robotics Research and Development Group, Convergent Technology Research and Development Department, Korea Institute of Industrial Technology, Ansan 15588, South Korea (e-mail: daehee@kitech.re.kr).

W. Kim is with the School of Energy Systems Engineering, Chung-Ang University, Seoul 06974, South Korea (e-mail: whkim79@cau.ac.kr).

M. Tomizuka is with the Department of Mechanical Engineering, University of California, Berkeley, CA 94720-1740 USA (e-mail: tomizuka@berkeley.edu).

Color versions of one or more of the figures in this paper are available online at http://ieeexplore.ieee.org.

Digital Object Identifier 10.1109/TMECH.2017.2764110

I. INTRODUCTION

ELECTROHYDRAULIC servo systems (EHSSs) are important in industrial automation applications, such as robots, aircraft actuators, and rolling mills, owing to their high power-to-weight ratio and their ability to rapidly generate high forces [1]. Various control methods were proposed to improve position/force control performance for EHSS. A robust, adaptive and repetitive digital tracking control was developed to compensate for the disturbance in [2]. Variable structure control methods were developed for controlling EHSS in [3] and [4]. Several control methods employing input–output linearization were proposed for control with compensation of the global nonlinearities of EHSSs [5]–[8]. Backstepping control methods that make use of the dynamic properties of the EHSS were proposed by using the strict feedback form of EHSS dynamics [9]–[14]. Nonlinear control methods based on the singular perturbation theory were proposed to provide robustness to the uncertainty of the effective bulk modulus [15], [16]. An adaptive integral robust controller was proposed to compensate for structured and unstructured uncertainties in a hydraulic rotary actuator [17]. A counterbalancing speed control issue of the closed hydrostatic drive hydraulic system was studied for the heavy transportation vehicle under long downslope [18]. A barrier Lyapunov func-

tion based nonlinear control method was proposed to guarantee position tracking error constraint for EHSSs [19].

Although these techniques have successfully improved the position and force control performance of EHSS, all of these methods require full-state feedback. Unfortunately, it is not always possible to measure the full state of the EHSS because of limitations imposed by cost and space. Generally, the position feedback can be obtained by a linear variable differential transformer (LVDT). The velocity can be obtained by the derivative of the high-resolution feedback, but it is not always possible to use the high-resolution sensor also. Furthermore, the pressure sensor measurement involves noise. To overcome this problem, several observer-based control methods were proposed [20]–[22]. In [20], only acceleration was estimated by the observer. A proportional integral observer was designed to estimate the full state [21]. Although the estimation performance was validated, closed-loop stability was not proven [20], [21]. Recently, an observer-based controller was proposed for the position tracking control of the EHSS [22]. In [22], the stability was proven under the assumption that the "sgn" function was approximated by "atan," "tanh," or "sigm" function.

Furthermore, nonlinear control methods require the derivative of the measured signals. It may amplify the ripples of the mechanical vibration or the measurement noise or both. Recently, a flatness-based control method was proposed to reduce the ripples [23]. Although the method reduced the ripples and improved the position tracking performance, it also requires full-state information.

In this paper, we propose a high-gain-observer-based integral sliding mode control for improving the position tracking performance of EHSSs. The proposed method consists of a high-gain observer and an integral sliding mode controller. The high-gain observer is designed to estimate the velocity and the load pressure using the position feedback. The stability is proven without the approximation of the "sgn" function in EHSS dynamics. The integral sliding mode controller is proposed to improve the position tracking performance. The EHSS dynamics is transformed into the normal form to utilize the flatness property of the system. The required derivatives of the state variables are obtained using the flatness property without the derivative of the measured signal. Thus, the position ripples can be reduced by the proposed method. Closed-loop stability is proven using the singular perturbation theory. The performance of the proposed method is validated via simulation and experiments. The results demonstrate that the proposed method reduces the position tracking error and position ripples.

II. Mathematical Model of EHSSs

Fig. 1 shows the structure of an EHSS. In many EHSS applications, valve dynamics is much faster than the dynamics of the remaining parts of the system. Therefore, valve dynamics often can be neglected without significant sacrifice of control performance [4], [8], [15], [16]. Therefore, for simplicity, we use the following approximation:

$$x_v = k_v i_v. \tag{1}$$

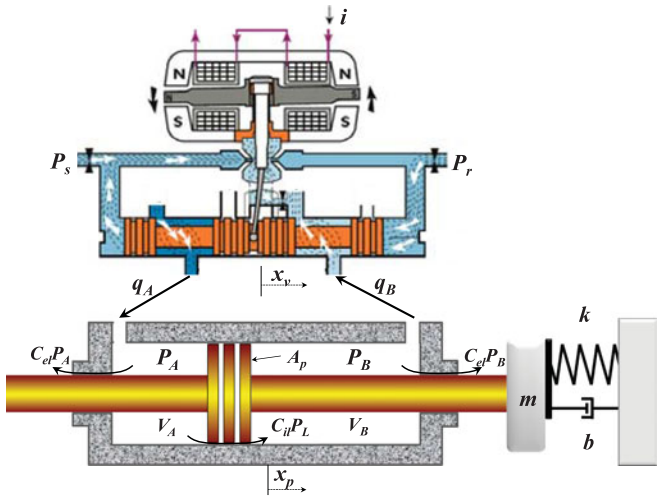

Fig. 1. Structure of an EHSS [24].

With the assumption that $|P_L| < P_s$ [1], the control flow equation of the hydraulic valve for the load flow rate can be written as

$$Q_L = C_d w x_v \sqrt{\frac{1}{\rho}(P_s - \mathrm{sgn}(x_v) P_L)}. \tag{2}$$

By applying the continuity law to each actuator chamber, the load flow rate continuity equation is given by [1]

$$Q_L = A_p \dot{x}_p + C_{tl} P_L + \frac{V_t}{4\beta_e} \dot{P}_L. \tag{3}$$

Combining the control flow rate equation (2) and the load flow rate continuity equation (3), the fluid dynamic equation of the actuator is given by

$$\dot{P}_L = -\frac{4\beta_e A_p}{V_t}\dot{x}_p - \frac{4\beta_e C_{tl}}{V_t} P_L + \frac{4\beta_e C_d w k_v}{V_t\sqrt{\rho}} \sqrt{(P_s - \mathrm{sgn}(x_v) P_L)} i_v. \tag{4}$$

Finally, by applying Newton's second law, the actuator's force balance equation is given by

$$m\ddot{x}_p = -k x_p - b\dot{x}_p + A_p P_L - f_l - f_f \tag{5}$$

where f_l and f_f are the load and the friction forces [N], respectively. Combining (1)–(5), the dynamics of the EHSSs can be formulated as the following state space representation [23]:

$$\begin{aligned} \dot{x}_1 &= x_2 \\ \dot{x}_2 &= -a_1 x_1 - a_2 x_2 + a_3 x_3 \\ \dot{x}_3 &= -h_1 x_2 - h_2 x_3 + h_3 \sqrt{P_s - \mathrm{sgn}(u)\, x_3} u \\ y &= x_1 \end{aligned} \tag{6}$$

where $x_1 = x_p$ is the position of the piston [m], $x_2 = \dot{x}_p$ is the velocity of the piston [m/s], $x_3 = P_L$ is the pressure difference between the chamber A and B [Pa], u is the current input [mA], and $a_1 := \frac{k}{m}$, $a_2 := \frac{b}{m}$, $a_3 := \frac{A_p}{m}$, $h_1 := \frac{4\beta_e A_p}{V_t}$, $h_2 := \frac{4\beta_e C_{tl}}{V_t}$, $h_3 := \frac{4\beta_e C_d w k_v}{V_t\sqrt{\rho}}$. The load force and friction, de-

noted by f_l and f_f, are, for all analysis purposes, assumed to be zero.

Remark 1: In practice, $\sqrt{P_s - \text{sgn}(u)x_3}$ is seldom imaginary number or zero, since $|x_3|$ is seldom higher than P_s. In the rare case that $P_s - \text{sgn}(u)x_3 \leq 0$, $\sqrt{P_s - \text{sgn}(u)x_3}$ is set to a small positive number in order to avoid the problem of dividing by imaginary number or zero [9]. ◊

III. High-Gain Observer Design

To derive a state observer for the system, we design a state observer to estimate the full state. The dynamics of the EHSS (6) can be written as

$$\begin{aligned} \dot{x} &= Ax + A_1(x) + \varphi(x,u) \\ y &= Cx \end{aligned} \tag{7}$$

where

$$A = \begin{bmatrix} 0 & 1 & 0 \\ 0 & 0 & a_3 \\ 0 & 0 & 0 \end{bmatrix}$$

$$A_1(x) = \begin{bmatrix} 0 \\ -a_1x_1 - a_2x_2 \\ -h_1x_2 - h_2x_3 \end{bmatrix}$$

$$\varphi(x,u) = \begin{bmatrix} 0 \\ 0 \\ h_3 u\sqrt{P_s - \text{sgn}(u)\,x_3} \end{bmatrix}$$

$$C = \begin{bmatrix} 1\,0\,0 \end{bmatrix}.$$

For the stability analysis, the EHSS dynamics are decomposed into Ax, $A_1(x)$, and $\varphi(x,u)$. As only position x_1 is available for measurement, to estimate the full state, we propose the following form of the state observer:

$$\dot{\hat{x}} = A\hat{x} + A_1(\hat{x}) + \varphi(\hat{x},u) + L(y - \hat{y}) \tag{8}$$

where $\hat{x}_i$, $i \in [1,3]$ is the estimation value of x_i, $L = [\frac{l_1}{\epsilon}, \frac{l_2}{\epsilon^2}, \frac{l_3}{\epsilon^3}]^T$ is the observer gain, and ϵ is a small positive constant. We define the estimation error as follows:

$$\tilde{x} = \begin{bmatrix} \tilde{x}_1 \\ \tilde{x}_2 \\ \tilde{x}_3 \end{bmatrix} = \begin{bmatrix} x_1 - \hat{x}_1 \\ x_2 - \hat{x}_2 \\ x_3 - \hat{x}_3 \end{bmatrix}. \tag{9}$$

The estimation error dynamics is given by

$$\dot{\tilde{x}} = A_o\tilde{x} + A_1(\tilde{x}) + \delta(x,\hat{x},u) \tag{10}$$

where

$$A_o = A - LC = \begin{bmatrix} -\frac{l_1}{\epsilon} & 1 & 0 \\ -\frac{l_2}{\epsilon^2} & 0 & a_3 \\ -\frac{l_3}{\epsilon^3} & 0 & 0 \end{bmatrix}$$

$$\begin{aligned} \delta(x,\hat{x},u) &= \varphi(x,u) - \varphi(\hat{x},u) \\ &= \begin{bmatrix} 0 \\ 0 \\ h_3\left(\sqrt{P_s - \text{sgn}(u)\,x_3} - \sqrt{P_s - \text{sgn}(u)\,\hat{x}_3}\right)u \end{bmatrix}. \end{aligned}$$

Let us define the scaled estimation error as

$$\begin{aligned} \eta &= \begin{bmatrix} \eta_1 & \eta_2 & \eta_3 \end{bmatrix}^T \\ &= \begin{bmatrix} \frac{1}{\epsilon^2}\tilde{x}_1 & \frac{1}{\epsilon}\tilde{x}_2 & \tilde{x}_3 \end{bmatrix}^T. \end{aligned} \tag{11}$$

Using the newly defined variable η, the estimation error dynamics (12) are transformed into a fast dynamics in a singularly perturbed form as

$$\epsilon\dot{\eta} = A_\eta\eta + A_1(\eta,\epsilon) + \epsilon\delta(x,\hat{x},u) \tag{12}$$

where the observer gains l_1, l_2, and l_3 are chosen such that

$$A_\eta = \begin{bmatrix} -l_1 & 1 & 0 \\ -l_2 & 0 & a_3 \\ -l_3 & 0 & 0 \end{bmatrix}$$

is Hurwitz. In (12), the term $\delta(x,\hat{x},u)$ can be rewritten as

$$\begin{aligned} \delta(x,\hat{x},u) &= \begin{bmatrix} 0 \\ 0 \\ -\frac{h_3|u|\tilde{x}_3}{\sqrt{P_s - \text{sgn}(u)x_3} + \sqrt{P_s - \text{sgn}(u)\hat{x}_3}} \end{bmatrix} \\ &= \begin{bmatrix} 0 \\ 0 \\ -\frac{h_3|u|\eta_3}{\sqrt{P_s - \text{sgn}(u)x_3} + \sqrt{P_s - \text{sgn}(u)\hat{x}_3}} \end{bmatrix} \\ &= \delta_\eta(\eta,x,\hat{x},u). \end{aligned} \tag{13}$$

Note that $\frac{h_3|u|}{\sqrt{P_s - \text{sgn}(u)x_3} + \sqrt{P_s - \text{sgn}(u)\hat{x}_3}}$ is always positive. Consequently, (12) becomes

$$\epsilon\dot{\eta} = A_\eta\eta + A_1(\eta,\epsilon) + \epsilon\delta_\eta(\eta,x,\hat{x},u). \tag{14}$$

In most cases, to satisfy the existence of the solution of x_3 and extend the control of EHSSs to bidirectional applications, the function $\text{sgn}(u)$ of the nonlinear term $\delta(x,\hat{x},u)$ is assumed to be a continuously differentiable function, $\text{atan}(ku)$, $\tanh(ku)$, or $\text{sigm}(x) = \frac{1-e^{-ax}}{1+e^{-ax}}$. However, in this paper, the stability of the state observer is analyzed without approximating the nonlinearity of the EHSSs.

Theorem 1: Consider the estimation error dynamics (14). If A_η is Hurwitz and ϵ is designed to satisfy the condition

$$0 < \epsilon < \frac{1}{2\lambda_{\max}(P_\eta)\gamma_{A_1}} \tag{15}$$

where P_η is a positive definite matrix and γ_Δ is a positive constant, then $\hat{x}$ goes to x by the high-gain observer, and $\lambda_{\max}(A)$ is the maximum eigenvalue of the matrix A, respectively. ◊

Proof: To study the convergence of the equilibrium points $\eta = 0$ of (14), we define a Lyapunov candidate function

$$V_\eta = \epsilon\eta^T P_\eta\eta. \tag{16}$$

Since A_η is Hurwitz, a positive definite matrix P_η exists such that

$$A_\eta^T P_\eta + P_\eta A_\eta = -I. \tag{17}$$

The derivative of V_η is

$$\dot{V}_\eta = -\eta^T\eta + 2\eta^T P_\eta A_1(\eta,\epsilon) + 2\epsilon\eta^T P_\eta\delta_\eta(\eta,x,\hat{x},u). \tag{18}$$

The term $P_\eta \delta_\eta(\eta, x, \hat{x}, u)$ on the right-hand side of (18) can be written as

$$P_\eta \delta_\eta(\eta, x, \hat{x}, u) = -P_\eta P_\delta(x, \hat{x}, u)\,\eta \tag{19}$$

where

$$P_\delta(x, \hat{x}, u) = \begin{bmatrix} 0 & 0 & 0 \\ 0 & 0 & 0 \\ 0 & 0 & \frac{h_3|u|}{\sqrt{P_s - \mathrm{sgn}(u)x_3} + \sqrt{P_s - \mathrm{sgn}(u)\hat{x}_3}} \end{bmatrix}.$$

Since γ_{A_1} exists satisfying

$$\begin{aligned} \|A_1(\eta, \epsilon)\|_2 &= \left\| \begin{bmatrix} 0 \\ -\epsilon^2 a_1 \eta_1 - \epsilon a_2 \eta_2 \\ -\epsilon^2 h_1 \eta_2 - \epsilon h_2 \eta_3 \end{bmatrix} \right\|_2 \\ &\le \epsilon \gamma_{A_1} \|\eta\|_2. \end{aligned} \tag{20}$$

We see that

$$\begin{aligned} \dot{V}_\eta &= -\eta^T \eta + 2\eta^T P_\eta A_1(\eta, \epsilon) - 2\epsilon \eta^T P_\eta P_\delta(x, \hat{x}, u)\,\eta \\ &\le -\|\eta\|_2^2 + 2\epsilon \lambda_{\max}(P_\eta)\gamma_{A_1}\|\eta\|_2^2 \\ &\le -(1 - 2\epsilon\lambda_{\max}(P_\eta)\gamma_{A_1})\|\eta\|_2^2. \end{aligned} \tag{21}$$

If $0 < \epsilon < \frac{1}{2\lambda_{\max}(P_\eta)\gamma_{A_1}}$, then $\dot{V}_\eta$ is negative definite. Therefore, the origin of (14) is exponentially stable. ■

IV. Controller Design

A. Flatness Property in Nonlinear Systems

Consider a nonlinear system

$$\dot{x} = f(x, u) \tag{22}$$

where x is the state and u is the input with the same dimensions as the output y. If there exists the output y

$$y = P(x, u, \dot{u}, \ldots, u^{(p)}) \tag{23}$$

such that x as well as u can be expressed as a function of y and a finite number of its time derivatives

$$x = Q(y, \dot{y}, \ldots, y^{(q)}) \tag{24}$$

$$u = R(y, \dot{y}, \ldots, y^{(q+1)}). \tag{25}$$

Then, (22) is called flat. The output y is called the flat output. The flatness property allows us to explicitly analyze the model by formally calculating the system variables as functions of the flat output and its time derivatives according to (24) and (25) [25].

B. Flatness Concept Application for EHSS

Let us define a flat output as

$$y = x_1. \tag{26}$$

Using (6) and (26), the states and the control input can be expressed as a function of the flat output y and a finite number of its time derivatives

$$\begin{aligned} x_1 &= y \\ x_2 &= \dot{y} \\ x_3 &= \frac{a_1 y + a_2 \dot{y} + \ddot{y}}{a_3} \\ u &= \frac{\phi\left(y, \dot{y}, \ddot{y}, y^{(3)}\right)}{\sqrt{a_3} h_3 \sqrt{P_s - \mathrm{sgn}\left(\phi\left(y, \dot{y}, \ddot{y}, y^{(3)}\right)\right)(a_1 y + a_2 \dot{y} + \ddot{y})}} \end{aligned} \tag{27}$$

where

$$\begin{aligned} \phi\left(y, \dot{y}, \ddot{y}, y^{(3)}\right) = a_1 h_2 y + (a_3 h_1 + a_2 h_2 + a_1)\,\dot{y} \\ + (a_2 + h_2)\,\ddot{y} + y^{(3)}. \end{aligned}$$

Hence, EHSS is differentially flat. This means that (27) represents the inverse dynamics of the original system (6). One can compute $(y, \dot{y}, \ddot{y})$ from (x_1, x_2, x_3) as follows:

$$\begin{aligned} y &= x_1 \\ \dot{y} &= x_2 \\ \ddot{y} &= -a_1 x_1 - a_2 x_2 + a_3 x_3. \end{aligned} \tag{28}$$

Consequently, $\dot{y}$ and $\ddot{y}$ can be obtained by using (28).

C. Integral Sliding Mode Controller Design

Our objective is to design a position tracking control using the full-state feedback to follow a given desired position trajectory y_d. Let us define new state variables as

$$\begin{aligned} z_1 &= x_1 \\ z_2 &= x_2 \\ z_3 &= -a_1 x_1 - a_2 x_2 + a_3 x_3. \end{aligned} \tag{29}$$

The original dynamics can be written in terms of new coordinates as

$$\begin{aligned} \dot{z}_1 &= z_2 \\ \dot{z}_2 &= z_3 \\ \dot{z}_3 &= f(z) + g(z, u)\,u \\ y &= z_1 \end{aligned} \tag{30}$$

where

$$\begin{aligned} f(z) &= -a_1 h_2 z_1 - (a_1 + a_2 h_2 + a_3 h_1) z_2 - (a_2 + h_2) z_3 \\ g(z, u) &= a_3 h_3 \sqrt{P_s - \mathrm{sgn}(u)\left(\frac{a_1 z_1 + a_2 z_2 + z_3}{a_3}\right)}. \end{aligned}$$

We define the tracking error $e = [e_0,\ e_1,\ e_2,\ e_3]^T$ as

$$\begin{aligned} e_0 &= \int_0^t e_1 d\tau \\ e_1 &= y_d - z_1 \\ e_2 &= \dot{y}_d - z_2 \\ e_3 &= \ddot{y}_d - z_3. \end{aligned} \tag{31}$$

The integrator is added for eliminating the steady-state error due to constant disturbance. From (30) and (31), we obtain the tracking error dynamics as follows:

$$\begin{aligned} \dot{e}_0 &= e_1 \\ \dot{e}_1 &= e_2 \\ \dot{e}_2 &= e_3 \\ \dot{e}_3 &= y_d^{(3)} - f(z) - g(z,u)\,u \end{aligned} \tag{32}$$

where $e_0 = \int_0^t e_1 \tau$. The sliding surface s is designed in terms of the error as

$$s = \sigma_0 e_0 + \sigma_1 e_1 + \sigma_2 e_2 + e_3 \tag{33}$$

where the coefficients σ_0, σ_1, and σ_2 are chosen such that the polynomial $s^3 + \sigma_2 s^2 + \sigma_1 s + \sigma_0 = 0$ is Hurwitz. From (33), we obtain $\dot{s}$ as

$$\begin{aligned} \dot{s} &= \sigma_0 \dot{e}_0 + \sigma_1 \dot{e}_1 + \sigma_2 \dot{e}_2 + \dot{e}_3 \\ &= \sigma_0 e_1 + \sigma_1 e_2 + \sigma_2 e_3 + \dot{e}_3 \\ &= \sigma_0 e_1 + \sigma_1 e_2 + \sigma_2 e_3 + y_d^{(3)} - f(z) - g(z,u)\,u. \end{aligned} \tag{34}$$

The control law is

$$u = \frac{-k_s \mathrm{sgn}(s) + y_d^{(3)} - \sigma_0 e_1 - \sigma_1 e_2 - \sigma_2 e_3 - f(z)}{g(z,u)} \tag{35}$$

where k_s is positive constant.

Theorem 2: Consider the tracking error dynamics (32). If the controller (35) is applied to the tracking error dynamics (32), then the tracking error e exponentially converges to zero. ♢

Proof: With the controller (35), s dynamics takes the form

$$\dot{s} = -k_s \mathrm{sgn}(s). \tag{36}$$

Thus, s exponentially converges to zero in finite time. With $s = 0$, the tracking error dynamics (32) is

$$\begin{bmatrix} \dot{e}_0 \\ \dot{e}_1 \\ \dot{e}_2 \end{bmatrix} = \underbrace{\begin{bmatrix} 0 & 1 & 0 \\ 0 & 0 & 1 \\ -\sigma_0 & -\sigma_1 & -\sigma_2 \end{bmatrix}}_{A_e} \begin{bmatrix} e_0 \\ e_1 \\ e_2 \end{bmatrix}. \tag{37}$$

Since the coefficients σ_0, σ_1, and σ_2 are chosen such that the polynomial $s^3 + \sigma_2 s^2 + \sigma_1 s + \sigma_0 = 0$, that is, A_e is Hurwitz, the tracking error e exponentially converges to zero. ■

Remark 2: It is important to note that $g(z)$ of (35) cannot be computed "as is," because it contains the control input u on both sides of an equation involving the sgn(·) function. We can see that sign of u is determined by the numerator term $u_b = -k_s \mathrm{sgn}(s) + y_d^{(3)} - \sigma_0 e_1 - \sigma_1 e_2 - \sigma_2 e_3 - f(z)$ because $g(z,u)$ is physically always greater than 0. ♢

The modified control law (35) takes the following form:

$$u = \frac{-k_s \mathrm{sgn}(s) + y_d^{(3)} - \sigma_0 e_1 - \sigma_1 e_2 - \sigma_e z_3 - f(z)}{g_m(z,u_b)} \tag{38}$$

where

$$g_m(z,u_b) = a_3 h_3 \sqrt{P_s - \mathrm{sgn}(u_b)\left(\frac{a_1 z_1 + a_2 z_2 + z_3}{a_3}\right)}.$$

Remark 3: Control method (38) requires that $\dot{y} = z_2$ and $\ddot{y} = z_3$. The derivative of the measured signals may amplify the ripples. From (28), $\dot{y}$ and $\ddot{y}$ can be obtained without using the derivative. ♢

V. Closed-Loop Stability Analysis Using Singular Perturbation Theory

The general standard full singular perturbed system [26], [27] is in the form of

$$\begin{aligned} \dot{x} &= f(t,x,z,\epsilon) \\ \epsilon \dot{z} &= g(t,x,z,\epsilon) \end{aligned} \tag{39}$$

where f and g are continuously differentiable and $x \in \mathbb{R}^n$ is the state of the slow subsystem, $z \in \mathbb{R}^m$ is the state of the fast subsystem, and ϵ is a small positive parameter. We use $x(t,\epsilon)$ and $z(t,\epsilon)$ to denote the solution of the full singular perturbation problem. The main idea of singular perturbation method is to divide the dynamics of the system into two separate time scales, so that the resulting design problem is easier to solve than the design problem of the full singularly perturbed system [26], [27]. It is assumed that $0 = g(t,x,z,0)$ has isolated real roots

$$\bar{z} = h(t,x). \tag{40}$$

The reduced-order system is defined as

$$\dot{x} = f(t,x,h(t,x),0). \tag{41}$$

$\bar{x}(t)$ is the solution of (41). And the quasi-steady-state is

$$\bar{z}(t) = h(t,\bar{x}(t)). \tag{42}$$

In order to shift the quasi-steady-state of z to the origin, we define y as

$$y = z - h(t,x). \tag{43}$$

With new time variable $\frac{d\tau}{dt} = \frac{1}{\epsilon}$, the boundary-layer system is obtained as

$$\frac{dy}{d\tau} = g(t,x,y+h(t,x),0) \tag{44}$$

where t and x are treated as fixed parameters.

In practice, since only the position x_1 is available for measurement, the controller (38) uses $\hat{x}$ instead of x. Thus, with $\hat{x}$, the control law (38) becomes

$$\hat{u} = \frac{-k_s \mathrm{sgn}(\hat{s}) + y_d^{(3)} - \sigma_0 \hat{e}_1 - \sigma_1 \hat{e}_2 - \sigma_2 \hat{e}_3 - f(\hat{z})}{g_m(\hat{z},\hat{u}_b)} \tag{45}$$

where $\hat{e}_1 = y_d - \hat{z}_1$, $\hat{e}_2 = \dot{y}_d - \hat{z}_2$, $\hat{e}_3 = \ddot{y}_d - \hat{z}_3$, $\hat{z}_i = \hat{x}_i \ i \in [1, 2]$, $\hat{z}_3 = -a_1\hat{x}_1 - a_2\hat{x}_2 + a_3\hat{x}_3$, $\hat{e}_0 = \int_0^t \hat{e}_1(\tau)d\tau$, $\hat{e}_j = y_d^{(j)} - \hat{z}_j \ \ j \in [1, 3]$, $\hat{s} = \sigma_0\hat{e}_0 + \sigma_1\hat{e}_1 + \sigma_2\hat{e}_2 + \hat{e}_3$, and $\hat{u}_b = -k_s\text{sgn}(\hat{s}) + y_d^{(3)} - \sigma_0\hat{e}_1 - \sigma_1\hat{e}_2 - \sigma_2\hat{e}_3 - f(\hat{z})$. Note that $\hat{u}$ is equal to u if $\hat{x}$ is equal to x. Actually, (45) is used instead of (38) in (34). Thus, from (34) and (45), s dynamics becomes

$$\dot{s} = -k_s\text{sgn}(s) + gu - g\hat{u}. \tag{46}$$

Consequently, the closed-loop system can be rewritten in the form of a singular perturbation model as follows:

$$\begin{aligned} \dot{s} &= -k_s\text{sgn}(s) + gu - g\hat{u} \\ \epsilon\dot{\eta} &= A_\eta\eta + A_1(\eta, \epsilon) + \epsilon\delta_\eta(\eta, x, \hat{x}, u). \end{aligned} \tag{47}$$

Theorem 3: Consider the singular perturbation problem of the closed-loop system (47). If A_η and A_e are Hurwitz, and k_s is positive constant, then there exists a positive constant ϵ^* such that for $0 < \epsilon < \epsilon^*$, the tracking error e decays exponentially. ◊

Proof: In (47), the equilibrium point of the η dynamics is the origin. With new time variable $\frac{d\tau}{dt} = \frac{1}{\epsilon}$, the boundary-layer system is obtained as

$$\frac{d\eta}{d\tau} = A_\eta\eta. \tag{48}$$

In Theorem 1, it was shown that the origin of the boundary-layer model (48) in (47) is exponentially stable with Hurwitz A_η. Therefore, $\hat{x}$ exponentially converge to quasi-steady-state x. Since $\hat{u}$ is equal to u in the quasi-steady-state, the reduced-order model (46) becomes

$$\dot{s} = -k_s\text{sgn}(s). \tag{49}$$

Earlier, in the discussion of Theorem 2, it was proven that s exponentially converges to zero in finite time. Finally, we conclude that the origins of the boundary-layer model and the reduced-order model are exponentially stable. Therefore, using [27, Th. 11.4], there exists a positive constant ϵ^* such that for $0 < \epsilon < \epsilon^*$, the tracking error e decays exponentially. Consequently, if A_e is Hurwitz, e exponentially converges to zero as proven in Theorem 2. ■

Remark 4: Theorem 3 shows that the proposed method guarantees that the origin of e is exponentially stable. Thus, if the disturbances, i.e., parameter uncertainties, load force, and/or friction can be regarded as the vanishing perturbation term, then the proposed method guarantees the robustness against the disturbances [27]. On the other hand, if the disturbances are in the form of the nonvanishing perturbation term, it is guaranteed that the position tracking error is globally uniformly ultimately bounded [27]. The detailed robustness analysis is the another problem and is beyond the scope of this paper, but is given in [2], [8], [11], and [17]. ◊

Fig. 2 shows the block diagram of the proposed method. The high-gain observer estimates full state using the position feedback. The integral sliding mode controller makes the control input using the estimated states.

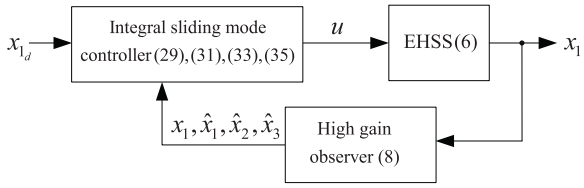

Fig. 2. Block diagram of the proposed method.

TABLE I
EHSSs AND CONTROLLER PARAMETERS

Parameter	Value	Parameter	Value
m	10	k	5000
b	1000	C_d	0.6
A_p	4.812×10^{-4}	β_e	1.8×10^9
V_t	6.2×10^{-5}	C_{il}	2.48815×10^{-14}
C_{el}	1.666×10^{-14}	w	5.2×10^{-3}
ρ	840	k_v	1.33×10^{-5}
P_s	12.0×10^6	σ_0	2.0×10^8
σ_1	2.3×10^6	σ_2	3.1×10^3
l_1	200	l_2	50
l_3	3.8110×10^8	ϵ	0.1
k_s	2		

VI. SIMULATIONS AND EXPERIMENTS

A. Simulation Results

To evaluate the position tracking and estimation performances of the proposed controller, simulations were performed using MATLAB/Simulink. Table I lists the parameters of the EHSSs (6) and controller (8), (35).[1] In order to study the robustness performance of the proposed method, the different values of the parameters were used in the EHSS (6) and the controller (8), (35). The parameter uncertainties were at most 10% of the nominal values in Table I. The desired position trajectory was $y_d = 0.02\sin(\pi \times t)$. In simulations, the load force and the friction were used as the disturbance. The friction model (50) given in [28] was used as follows:

$$f_f(x_2) = f_v x_2 + \text{sgn}(x_2)\left[f_{c0} + f_{s0}e^{-(\frac{x_2}{c_s})^2}\right] \tag{50}$$

where f_v is the viscous coefficient, f_{c0} is the parameter for Coulomb friction, and f_{s0} and c_s are the parameters for static coefficient, respectively.

1) Sinusoidal Reference Tracking and Estimation Performances: Fig. 3 shows the position tracking performance of the proposed output feedback control with sinusoidal reference. We see that the position of the EHSS matched the desired position trajectory well. The peaking in the position appeared near zero velocity due to the friction. Although the disturbance including the parameter uncertainties the friction, and the load force exited, the position tracking error was less than 1% of the desired position. Fig. 4 shows the estimation performances of the position, velocity, and load pressure. The estimated state variable

[1]The EHSS parameter values were supplied by the manufacturer at the request of the authors.

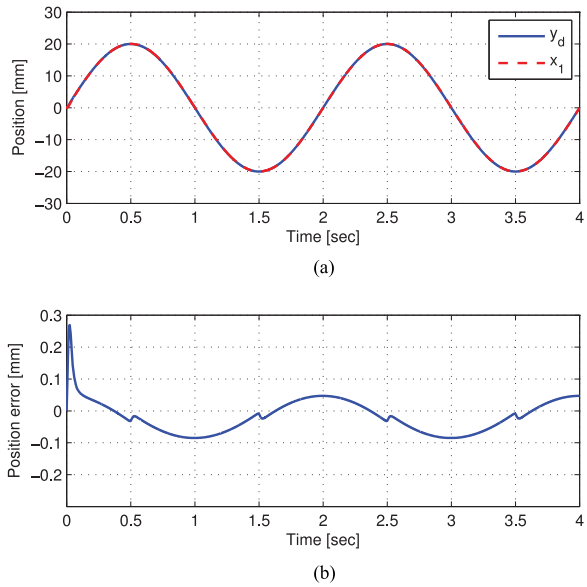

Fig. 3. Position tracking performance of the proposed method. (a) Position tracking performance. (b) Position tracking error.

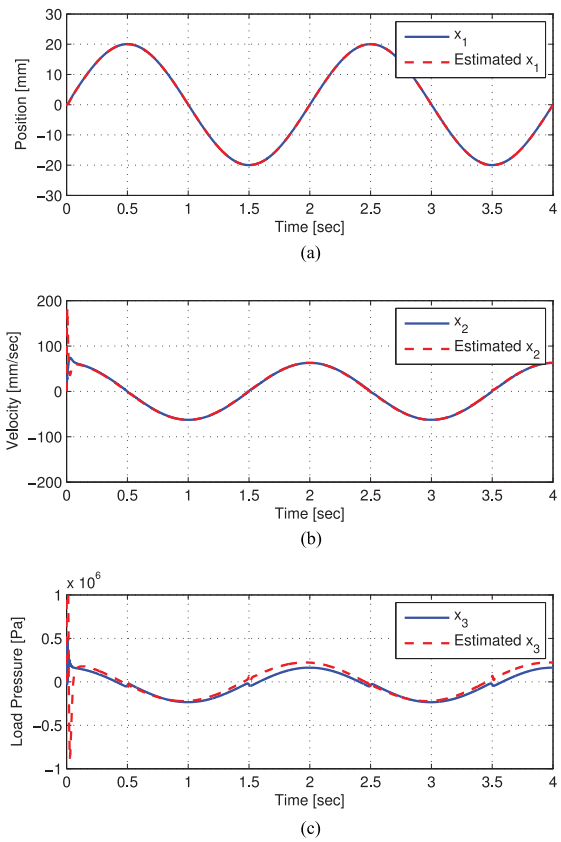

Fig. 4. Estimation results of the proposed state observer. (a) Estimation of x_1. (b) Estimation of x_2. (c) Estimation of x_3.

tracked the actual state variables well in the position and the velocity estimations. In the load pressure estimation, the relatively small estimation errors were caused by the disturbance in the load pressure estimations.

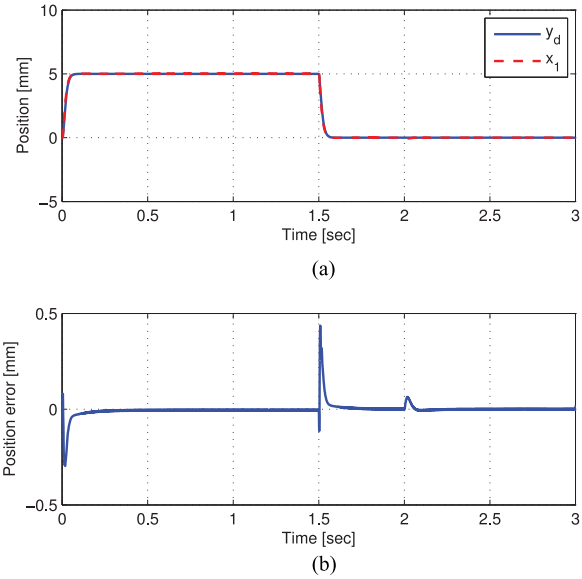

Fig. 5. Position tracking performance of the proposed method. (a) Position tracking performance. (b) Position tracking error.

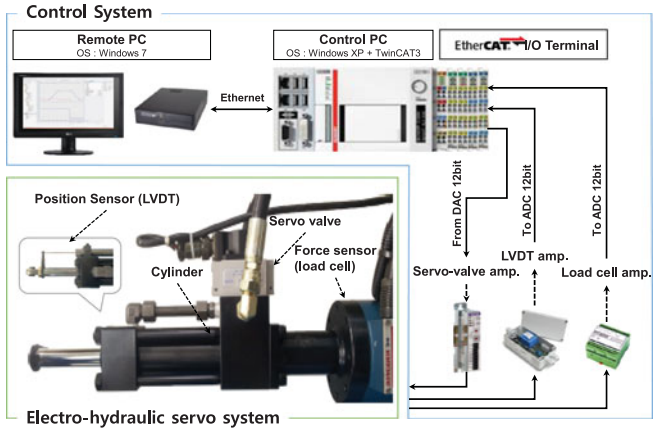

Fig. 6. Experimental setup of an EHSS.

2) Step Reference With Step Load Force Disturbance: Fig. 5 shows the position tracking performance of the proposed output feedback control with step reference. To evaluate the position tracking performance of the proposed method under a sudden disturbance, the step load force disturbance occurred at 2 s. The position tracking error had a peak due to the step disturbance at 2 s. Since the integral action in (33) and "sgn" function in (35) suppressed the disturbance, the position tracking error converged to zero. Consequently, it is observed that the position of the EHSS matched the desired position trajectory well.[2]

B. Experimental Results

The experiments were executed to evaluate the performance of the proposed method. Fig. 6 shows the experimental setup. A flapper-type servo valve M454 manufactured by Star Hy-

[2]These simulations were performed to study the position tracking performance under the sudden disturbance. The detailed stability analysis under the sudden disturbance is beyond the scope of this paper.

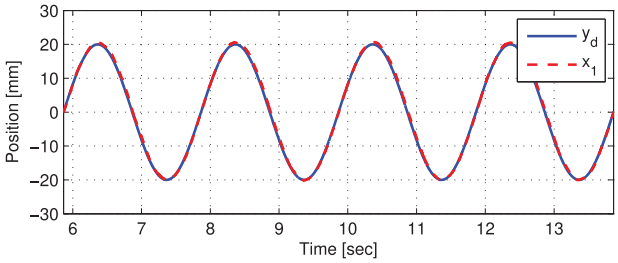

(a)

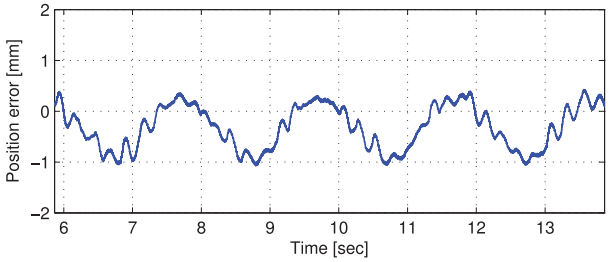

(b)

Fig. 7. Position tracking performance of the backstepping controller. (a) Position tracking performance. (b) Position tracking error.

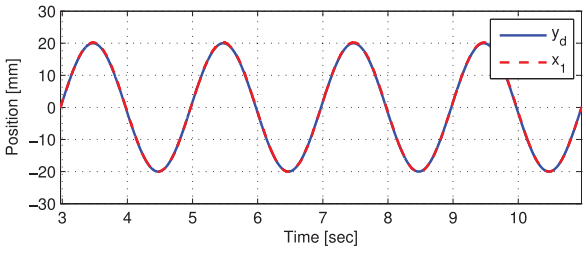

(a)

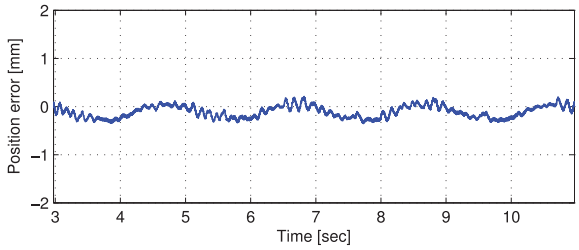

(b)

Fig. 8. Position tracking performance of the proposed method. (a) Position tracking performance. (b) Position tracking error.

draulic Ltd., was used. The effective stroke length of the piston was ± 0.043 m. The position was measured by the LVDT. The force cell was used to measure the force and to validate the estimation performance of the load pressure. The velocity is numerically approximated by differentiating the position measurement using the forward Euler method. The control law was programmed in *C* language. Real-time implementation of the controller was conducted at a sampling rate of 1 kHz by using a 12-bit analog-to-digital converter and digital-to-analog converter with EtherCAT interface and using an Intel Dual Core 2.16 GHz processor C6920 with extended automation system TwinCAT 3. We compared the performances of the proposed

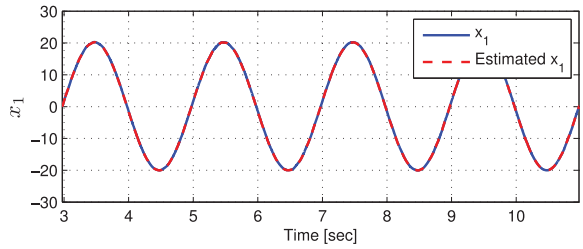

(a)

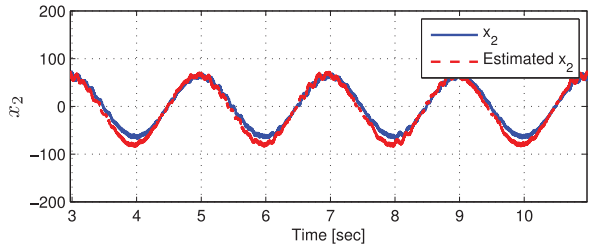

(b)

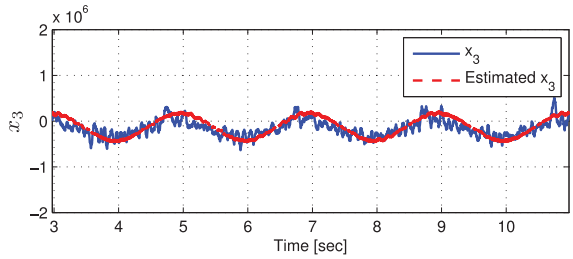

(c)

Fig. 9. Estimation results of the proposed state observer. (a) Estimation of x_1. (b) Estimation of x_2. (c) Estimation of x_3.

method and the backstepping controller. For the experiments, in order to validate the performance of the integral sliding mode control (34), the backstepping controller (51) with the high-gain observer (8) was designed as follows:

$$u = \frac{h_1 x_2 + h_2 x_3 - k_{c3}\xi_3 - a_3\xi_2 + y_d^{(3)} + \dot{\alpha}_2}{h_3\sqrt{P_s - \text{sgn}(u_b)x_3}} \tag{51}$$

where

$$\xi_1 = x_1 - y_d,\ \xi_2 = x_2 - \dot{y}_d - \alpha_1,\ \xi_3 = x_3 - \ddot{y}_d - \alpha_2$$

$$\alpha_1 = -k_{c1}\xi_1$$

$$\alpha_2 = \frac{a_1 x_1 + a_2 x_2 - k_{c2}\xi_2 - \xi_1 - (a_3 - 1)\ddot{y}_d + \dot{\alpha}_1}{a_3}$$

$$u_b = h_1 x_2 + h_2 x_3 - k_{c3}\xi_3 - a_3\xi_2 + y_d^{(3)} + \dot{\alpha}_2$$

$k_{c1} = 200$, $k_{c2} = 1000$, and $k_{c3} = 130$.

Figs. 7 and 8 show the position tracking performances of both methods. In the case of the backstepping controller, the position tracking error was asymmetric because of load force disturbance. The position tracking error was less than 5% of the desired position. The position ripples due to mechanical vibration increased because the derivatives of the measured signals were used. In the proposed method, the position tracking error was less than 2% of the desired position. The position

tracking error of the proposed method was less than 40% of the error of the backstepping controller. The phase lag was also reduced by the proposed method. Furthermore, the position ripples were reduced because the proposed method did not require any derivatives of the state variables. Fig. 9 shows the estimation performances of the proposed method. The estimated state variables tracked the actual state variables well, however, the relatively small offset estimation errors were caused by the disturbance including the parameter uncertainties the friction, and the load force in the velocity and load pressure estimations. In spite of the offset estimation errors in the velocity and load pressure estimation, the proposed method improved the position tracking performance.

VII. Conclusion

We proposed a high-gain-observer-based integral sliding mode control for the position tracking of EHSSs. The high-gain observer was designed to estimate the velocity and load pressure by using the position feedback. The integral sliding mode controller was developed to improve the position tracking performance. The proposed method does not require any derivatives of the state variables. Closed-loop stability was proven using the singular perturbation theory. The performance of the proposed method was validated via simulations and experiments. The proposed controller was compared to the backstepping controller. The results indicated that the proposed method reduced the position tracking error and position ripples.

References

[1] H. E. Merrit, *Hydraulic Control System.* New York, NY, USA: Wiley, 1967.

[2] T.-C. Tsao and M. Tomizuka, "Robust adaptive and repetitive digital tracking control and application to a hydraulic servo for noncircular machining," *J. Dyn. Syst. Meas. Control*, vol. 116, no. 1, pp. 24–32, 1994.

[3] A. Alleyne and J. K. Hedrick, "Nonlinear adaptive control of active suspensions," *IEEE Trans. Control Syst. Technol.*, vol. 3, no. 1, pp. 94–101, Mar. 1995.

[4] M. Jerouane, N. Sepehri, and F. Lamnabhi-Lagarriguea , "Dynamic analysis of variable structure force control of hydraulic actuators via the reaching law approach," *Int. J. Control*, vol. 77, no. 4, pp. 1260–1268, 2004.

[5] H. Hahn, A. Piepenbrink, and K.-D. Leimbach, "Input/output linearization control of an electro servo-hydraulic actuator," in *Proc. 3rd IEEE Int. Conf. Control Appl.*, 1994, pp. 995–1000.

[6] G. Vossoughi and M. Donath, "Dynamic feedback linearization for electrohydraulically actuated control systems," *J. Dyn. Syst. Meas. Control*, vol. 117, pp. 468–477, 1995.

[7] J. Seo, R. Venugopala, and J.-P. Kenn, "Feedback linearization based control of a rotational hydraulic drive," *Control Eng. Pract.*, vol. 15, no. 12, pp. 1495–1507, 2007.

[8] W. Kim, D. Shin, D. Won, and C. C. Chung, "Disturbance observer based position tracking controller in the presence of biased sinusoidal disturbance for electro-hydraulic actuators," *IEEE Trans. Control Syst. Technol.*, vol. 21, no. 6, pp. 2290–2298, Nov. 2013.

[9] A. Alleyne and R. Liu, "A simplified approach to force control for electro-hydraulic systems," *Control Eng. Pract.*, vol. 8, no. 12, pp. 1347–1356, 2000.

[10] M. R. Sirouspour and S. E. Salcudean, "On the nonlinear control of hydraulic servo-systems," in *Proc. IEEE Int. Conf. Robot. Autom.*, 2000, pp. 1276–1282

[11] B. Yao, F. Bu, J. Reedy, and G. T. C. Chiu, "Adaptive robust motion control of single-rod hydraulic actuators: Theory and experiments," *IEEE/ASME Trans. Mechatronics*, vol. 5, no. 1, pp. 79–91, Mar. 2000.

[12] C. Kaddissi, J.-P. Kenné, and M. Saad, "Identification and real-time control of an electrohydraulic servo system based on nonlinear backstepping," *IEEE/ASME Trans. Mechatronics*, vol. 12, no. 1, pp. 12–22, Feb. 2007.

[13] C. Guan and S Pan, "Adaptive sliding mode control of electro-hydraulic system with nonlinear unknown parameters," *Control Eng. Pract.*, vol. 16, no. 11, pp. 1275–1284, 2008.

[14] C. Kaddissi, J.-P. Kennè, and M. Saad, "Indirect adaptive control of an electrohydraulic servo system based on nonlinear backstepping," *IEEE/ASME Trans. Mechatronics*, vol. 16, no. 6, pp. 1171–1177, Dec. 2012.

[15] B. Eryilmaz and B. H. Wilson, "Improved tracking control of hydraulic systems," *J. Dyn. Syst. Meas. Control*, vol. 123, pp. 457–462, 2001.

[16] L. Wang, W. J. Book, and J. D. Huggins, "Application of singular perturbation theory to hydraulic pump controlled systems," *IEEE/ASME Trans. Mechatronics*, vol. 17, no. 2, pp. 251–259, Apr. 2012.

[17] J. Yao, Z. Jiao, D. Ma, and L. Yan, "High-accuracy tracking control of hydraulic rotary actuators with modeling uncertainties," *IEEE/ASME Trans. Mechatronics*, vol. 19, no. 2, pp. 633–641, Apr. 2014.

[18] Y. Li and L. He, "Counterbalancing speed control for hydrostatic drive heavy vehicle under longdown-slope," *IEEE/ASME Trans. Mechatronics*, vol. 20, no. 4, pp. 1533–1542, Aug. 2015.

[19] D. Won, W. Kim, D. Shin, and C. C. Chung, "High-gain disturbance observer-based backstepping control with output tracking error constraint for electro-hydraulic systems," *IEEE Trans. Control Syst. Technol.*, vol. 23, no. 2, pp. 787–795, Mar. 2015.

[20] F. Bu and B. Yao, "Observer based coordinated adaptive robust control of robot manipulators driven by single-rod hydraulic actuators," in *Proc. IEEE Int. Conf. Robot. Autom.*, 2000, pp. 3034–3039.

[21] P. Nakkarat and S. Kuntanapreeda, "Observer-based backstepping force control of an electro hydraulic actuator," *Control Eng. Pract.*, vol. 17, no. 8, pp. 895–902, 2009.

[22] W. Kim, D. Won, D. Shin, and C. C. Chung, "Output feedback nonlinear control for electro-hydraulic systems," *Mechatronics*, vol. 22, no. 6, pp. 766–777, 2012.

[23] W. Kim, D. Won, and M. Tomizuka, "Flatness based nonlinear control for position tracking of electro-hydraulic systems," *IEEE/ASME Trans. Mechatronics*, vol. 20, no. 1, pp. 197–206, Feb. 2015.

[24] Moog, "Electrohydraulic valves... a technical look," [Online]. Available: http://www.moog.com/literature/ICD/Valves-Introduction.pdf

[25] M. Fliess, J. Lévine, P. Martin, and P. Rouchon, "Flatness and defect of non-linear systems: Introductory theory and examples," *Int. J. Control*, vol. 61, no. 6, pp. 1327–1361, 1995.

[26] P. Kokotovic, H. Khalil, and J. O'Reilly, *Singular Perturbation Methods in Control: Analysis and Design.* New York, NY, USA: Academic, 1991 (republished by SIAM, 1986).

[27] H. Khalil, *Nonlinear Systems*, 3rd ed. Englewood Cliffs, NJ, USA: Prentice-Hall, 2002.

[28] B. Armstrong-Helouvry, P. Dupont, and C. C. de Wit, "A survey of models, analysis tools and compensation methods for the control of machines with friction," *Automatica*, vol. 30, no. 7, pp. 1083–1138, 1994.

Daehee Won (M'16) received the B.S. degree in control and instrumentation engineering from Korea University, Sejong, South Korea, and the M.S. degree in precision mechanical engineering and the Ph.D. degree in electrical engineering from Hanyang University, Seoul, in 2000, 2002, and 2015, respectively.

Since 2003, he has been with the Robotics Research and Development (R&D) Group, Convergent Technology R&D Department, Korea Institute of Industrial Technology, Ansan, South Korea. From 2005 to 2006, he was part of the Robot Team, Ministry of Commerce Industry and Energy, Seoul. His research interests include nonlinear control, robot control, real-time motion network, and electro-hydraulic applications.

Wonhee Kim (S'09–M'12) received the B.S. and M.S. degrees in electrical and computer engineering, and the Ph.D. degree in electrical engineering from Hanyang University, Seoul, South Korea, in 2003, 2005, and 2012, respectively.

From 2005 to 2007, he was at Samsung Electronics Company, Suwon, South Korea. In 2012, he was at the Power and Industrial Systems Research and Development Center, Hyosung Corporation, Seoul. In 2013, he was a Postdoctoral Researcher at the Institute of Nano Science and Technology, Hanyang University, and a Visiting Scholar in the Department of Mechanical Engineering, University of California, Berkeley, CA, USA. From 2014 to 2016, he was in the Department of Electrical Engineering, Dong-A University, Busan, South Korea. He is currently an Assistant Professor with the School of Energy Systems Engineering, Chung-Ang University, Seoul. His research interests include nonlinear control and nonlinear observers, as well as their industrial applications.

Masayoshi Tomizuka (M'86–SM'95–F'97–LF'17) received the B.S. and M.S. degrees in mechanical engineering from Keio University, Tokyo, Japan, in 1968 and 1970, respectively, and the Ph.D. degree in mechanical engineering from the Massachusetts Institute of Technology, Cambridge, MA, USA, in 1974, after which he joined the ME Department at UC Berkeley.

In 1974, he joined the Department of Mechanical Engineering, University of California at Berkeley, Berkeley, CA, USA, where he is currently the Cheryl and John Neerhout, Jr. Distinguished Professor. He teaches courses on dynamic systems and controls, and conducts research on optimal and adaptive control, digital control, and motion control and their applications to robotics, manufacturing, information storage devices, and vehicles. He was the Program Director of the Dynamic Systems and Control Program of the Civil and Mechanical Systems Division, National Science Foundation (2002–2004).

Dr. Tomizuka was the Technical Editor of the *ASME Journal of Dynamic Systems, Measurement, and Control* (1988–1993), and the Editor-in-Chief of the IEEE/ASME TRANSACTIONS ON MECHATRONICS (1997–1999). He is a Life Fellow of the American Society of Mechanical Engineers (ASME), the International Federation of Automatic Control, and the *Society of Manufacturing Engineers*. He received the Charles Russ Richards Memorial Award (ASME, 1997), the Rufus Oldenburger Medal (ASME, 2002), and the John R. Ragazzini Award (American Automatic Control Council, 2006).